



## **An intelligent optimization method for the facility environment on rural roads**

Downloaded from: <https://research.chalmers.se>, 2024-06-30 08:55 UTC

Citation for the original published paper (version of record):

Ren, W., Yu, B., Chen, Y. et al (2024). An intelligent optimization method for the facility environment on rural roads. *Computer-Aided Civil and Infrastructure Engineering*, In Press. <http://dx.doi.org/10.1111/mice.13209>

N.B. When citing this work, cite the original published paper.



# An intelligent optimization method for the facility environment on rural roads

Weixi Ren<sup>1</sup> | Bo Yu<sup>1</sup> | Yuren Chen<sup>1</sup> | Kun Gao<sup>2</sup> | Shan Bao<sup>3,4</sup> | Zhixuan Wang<sup>1</sup> | Yuting Qin<sup>1</sup>

<sup>1</sup>Key Laboratory of Road and Traffic Engineering of the Ministry of Education, College of Transportation Engineering, Tongji University, Shanghai, China

<sup>2</sup>Department of Architecture and Civil Engineering, Chalmers University of Technology, Gothenburg, Sweden

<sup>3</sup>Industrial and Manufacturing Systems Engineering Department, University of Michigan, Dearborn, Michigan, USA

<sup>4</sup>Human Factors Group, University of Michigan Transportation Research Institute, Michigan, USA

## Correspondence

Bo Yu, Key Laboratory of Road and Traffic Engineering of the Ministry of Education, College of Transportation Engineering, Tongji University, 4800 Cao'an Highway, Shanghai 201804, China.  
Email: [boyu@tongji.edu.cn](mailto:boyu@tongji.edu.cn)

Kun Gao, Department of Architecture and Civil Engineering, Chalmers University of Technology, SE-412 96 Gothenburg, Sweden.  
Email: [gkun@chalmers.se](mailto:gkun@chalmers.se)

## Funding information

National Natural Science Foundation of China, Grant/Award Number: 52102416; Natural Science Foundation of Shanghai, Grant/Award Number: 22ZR1466000

## Abstract

This study develops an intelligent optimization method of the facility environment (i.e., road facilities and surrounding landscapes) from drivers' visual perception to adjust operation speeds on rural roads. Different from previous methods that heavily rely on expert experience and are time-consuming, this method can rapidly generate optimized visual images of the facility environment and promptly verify the optimization effects. In this study, a visual road schema model is established to quantify the facility environment from drivers' visual perception, and an automated optimization scheme determination approach considering the original facility environment characteristics is proposed using self-explaining theory. Then, Cycle-consistent generative adversarial network is used to automatically generate optimized facility environment images. To verify the optimization effect, operation speeds of the optimized facility environments are predicted using random forest. The case study shows that this method can effectively optimize the facility environment where original operation speeds are more than 20% over the speed limits, and the whole process only takes 1 h far less than several months or years in previous ways. Overall, this study advances the intelligence level in optimizing the facility environment and enhances rural road safety.

## 1 | INTRODUCTION

Regardless of small traffic volumes, crashes on rural roads are still frequent and severe (Marshall & Ferenchak, 2017). In the United States, 43% of all traffic fatalities in 2020

happened in rural areas, even though only 19% of the population lived in rural areas. The fatality rate per 100 million vehicle miles traveled on rural roads was 1.7 times higher than that on urban roads (NHTSA, 2022a). In China, according to the Traffic Administration Bureau of the

This is an open access article under the terms of the [Creative Commons Attribution](https://creativecommons.org/licenses/by/4.0/) License, which permits use, distribution and reproduction in any medium, provided the original work is properly cited.

© 2024 The Authors. *Computer-Aided Civil and Infrastructure Engineering* published by Wiley Periodicals LLC on behalf of Editor.

Ministry of Public Security of PRC (2020), the fatality rate on rural roads exceeded 60% in 2020, significantly higher than the urban road fatality rate of 35%. In Europe, 53% of road fatalities happened on rural roads in 2018, compared to 38% on urban roads and just 9% on freeways (EU Road Safety Statistics, 2019). Speeding is one of the major contributors to crashes on rural roads (Yu et al., 2019). In New Zealand, speeding was responsible for approximately 70% of injury crashes and around 60% of fatal crashes on rural roads (Job & Brodie, 2022). Besides, in the United States, speeding-related crashes claimed the lives of 4717 people, constituting 28% of rural traffic fatalities (NHTSA, 2022b). Therefore, there is widespread concern and critical demand to reduce speeding on rural roads.

Speeding is risky behavior of human drivers that consists of various interacting influencing factors, such as surrounding vehicles, road geometry, traffic enforcement, and facility environments (i.e., road facilities and surrounding landscapes; Ambunda & Sinclair, 2022). However, on rural roads, due to low traffic volume, vehicles often operate in a state of free-flow with little influence from surrounding vehicles (Gayah & Donnell, 2021). Besides, hindered by limited surrounding land use and capital investment capacity, the space for geometric design improvement is constrained on rural roads (Coakley et al., 2016; M. Xu et al., 2023). Furthermore, the extensive coverage and complex surroundings of rural roads, coupled with limited financial and human resources, make traffic enforcement a formidable task (Shaaban et al., 2023). There is increasing acknowledgment that the layout of facility environments of rural roads has significant effects on drivers' speed selection, and optimizing the facility environments has become a vital approach to reduce speeding-related crashes on rural roads (Pasindu et al., 2021).

Self-explaining theory is a design concept of facility environments, which indicates that the layout of the facility environment should automatically elicit appropriate driving speeds (Theeuwes & Godhelp, 1995). Drivers make cognition toward road supply by perceiving facility environments and then select driving speeds accordingly (Theeuwes & van der Horst, 2017). When the road supply is appropriate, even with limited traffic enforcement on rural roads, drivers tend to adhere to the speed limits and select appropriate driving speeds (Charlton et al., 2010). The self-explaining theory focuses on using traffic signs, road markings, landscapes, and other semantics, to create facility environments that evoke drivers' correct cognition toward road supply (Theeuwes, 2021). Since it came out, the self-explaining theory has rapidly gained popularity (Ghorbani et al., 2023). For example, Germany has incorporated the self-explaining theory into their national guidelines for rural roads, emphasizing the importance of standardized and self-explanatory road design (Weber & Hartkopf, 2005). In 2017, the Czech Republic employed the

self-explaining theory to enhance safety on their national roads, and in 2019, Belarus adopted this theory to develop a new road traffic safety concept (Ambros et al., 2017; Kapsky et al., 2020).

Despite the widespread acceptance of the self-explaining theory, practical optimization of facility environments continues to encounter several challenges, including heavy reliance on expert experience, limited automation, and difficulties in prompt optimization effect verification (Naveen et al., 2017). This study aims to develop an intelligent optimization method of the facility environment from drivers' visual perception to adjust operation speeds on rural roads. In this study, a visual road schema model is established to quantify the facility environment from drivers' visual perception and an automated optimization scheme determination method is proposed using self-explaining theory. Then, the Cycle-consistent generative adversarial network (i.e., CycleGAN) is used to generate optimized facility environment images. Combined with the operation speed prediction model, the optimization effect could be verified promptly. The intelligent optimization method proposed in this study follows the concept of "human-oriented" and is conducive to achieving the function of facility environments in evoking accurate driver expectations of road categories and guiding most drivers to follow speed limits (i.e., the "self-explaining" function) of rural roads. Besides, this study will improve the degree of automation and intelligence in optimizing the facility environment and help reduce repetitive human work and the dependence on expert experience during road design.

## 2 | LITERATURE REVIEW

### 2.1 | Current facility environment optimization practice on rural roads

Currently, several studies have focused on reducing speeding on rural roads through the optimization of facility environments. Table 1 offers a literature review of these studies, summarizing the following key aspects: (1) targeted road sections; (2) facility environment semantics optimized in each study; (3) installation method (i.e., facility environment semantics were installed individually or in combination); (4) whether the analysis considered the original facility environment; (5) optimization effect; and (6) the method and time required for verifying the optimization effect.

From Table 1, it is evident that current facility environment optimization research typically follows a similar process. Designers or experts propose various road facilities designed to reduce operation speeds. These facilities are then implemented individually or in combinations on the targeted rural road sections based on engineering



TABLE 1 Summary of the facility environment optimization practice on rural roads.

Study	Targeted road section	Optimized semantics	Installation method	Consideration of the original facility environment	Optimization effect verification	
					Optimization effect	Method Time
Persaud et al. (2004)	Rural roads with frequent crashes	Centerline rumble strips	Individually	No	Crashes reduced by 12% on average	Collect crash data after installation More than 1 year
Herrstedt (2006)	Two-way two-lane rural roads with frequent crashes	Zone boards, edge markings and speed humps	In combination	No	Casualty crashes reduced by 24% on average	Collect crash data after installation More than 5 years
Hallmark et al. (2008)	Selected test major roads	Speed feedback signs and center islands	Individually	No	Both treatments successfully reduced operation speeds	Collect driving data after installation More than 1 year
Galante et al. (2010)	Rural roads with high operation speeds	Transverse rumble strips, roadside fences, colored brick strips	In combination	No	Driving speeds decrease by more than 10 km/h	Collect driving data with driving simulation Unknown
P. Liu et al. (2011)	Rural roads with frequent crashes	Transverse rumble strips	Individually	No	Driving speeds decrease in most roads by about 10 km/h	Collect driving data after installation About 2 years
Montella et al. (2011)	General rural road sections	Transverse rumble strips, peripheral transverse bars, dragon teeth markings, and so forth	Individually	No	Driving speeds on various sections decreased by 13–23 km/h	Collect driving data with driving simulation Unknown
Yuan et al. (2012)	General rural road sections	Horizontal, transverse and peripheral pavement markings	Individually	No	Operation speeds reduce by 6.6 km/h	Collect driving data after installation About 4 years
Mackie et al. (2017)	Rural intersections with frequent crashes	Road electronic signs, VSL signs, and so forth	In combination	No	Crashes were almost eliminated	Collect driving data after installation About 3 year
Babić and Brijis (2021)	Horizontal curves on rural roads with frequent crashes	Red median and horizontal warning signs	Individually	No	Both treatments successfully reduced operation speeds	Collect driving data with driving simulation Unknown
Mahmud et al. (2023)	Rural roads with high operation speeds	Dynamic speed feedback signs	Individually	No	Operation speeds decreased by 3.2 to 7.8 mph, and drivers were 78.8% to 92.4% less likely to speed	Collect driving data after installation About 1 year

experiences. Then, crashes or operation data from these sections are collected over a period ranging from several months to years, which enables the comparative analysis of the optimization effects. Undoubtedly, these studies have achieved advancements in reducing speeding and enhancing rural road safety. However, existing research still exhibits some limitations.

First, most study primarily concentrates on analyzing one or two categories of semantics, resulting in a limited scope for proposing facility environment optimization methods. Facility environments on rural roads encompass a variety of semantic categories, such as lane markings, traffic signs, roadside protections, and landscapes (L. He et al., 2023). A comprehensive consideration of these semantics would enhance the diversity of facility environment optimization methods.

Moreover, current research overlooks the characteristics of the original facility environments on different road sections. All targeted road sections with similar historical crash rates or operation speeds are treated uniformly and optimized in the same way. It remains uncertain how to propose the most effective optimization methods for different facility environments (Turner et al., 2017).

Additionally, verifying the optimization effect of the facility environment needs to build virtual scenarios within driving simulators or to conduct practical driving experiments on real roads, both of which are highly time-consuming processes. It is expected that once facility environment optimization methods are proposed, their effect could be timely estimated before implementation on the road (Yang et al., 2021). This prompt verification is crucial for enhancing efficiency and reducing the consumption of human and material resources in engineering practice (de Oña et al., 2014).

## 2.2 | Facility environment semantics affecting drivers' speed selection on rural roads

At present, numerous studies have analyzed the facility environment semantics that influence drivers' speed selection on rural roads. Table 2 offers a literature review of these studies, summarizing the following key aspects: (1) facility environment semantics analyzed in each study; (2) whether the analysis comprehensively considers various facility environment semantics; (3) the property of the results (i.e., qualitative or quantitative); (4) specific findings; and (5) whether the analysis considered drivers' visual perception.

Identifying the facility environment semantics that influence drivers' speed selection is the prerequisite for determining facility environment optimization schemes

(Walker et al., 2013). However, there are still certain limitations in the existing studies.

Some studies have conducted a comprehensive analysis of multiple semantics within the facility environment, identifying significant semantics on drivers' speed selection, such as trees and barriers (Antonson et al., 2014; Cruzado & Donnell, 2010; Cox et al., 2017; Yu et al., 2019). However, these analyses are often qualitative and lack quantitative assessments of the speed revision abilities of these semantics, making it challenging to provide theoretical support for determining applicable optimization schemes for facility environments. Conversely, other studies have quantified the speed revision abilities of specific facility environment semantics (Goldenbeld & van Schagen, 2007; Montella et al., 2015; Qin et al., 2020; Vignali et al., 2019). Nonetheless, these studies only account for cases in which a single facility environment semantic is present, leaving the effects of interactions and combinations of different semantics unknown. Currently, there is a lack of comprehensive investigation to quantitatively analyze the influence of various facility environment semantics on drivers' speed selection.

Drivers' speed selection is mainly determined by the driver's visual perception of the facility environment rather than the actual one (Yu et al., 2018). Previous studies have found a significant distinction between perceived and actual facility environment semantics (Du et al., 2018). Quantifying the facility environment from drivers' visual perception can help accurately analyze its impact on drivers' speed selection, thus improving the effectiveness and practicality of facility environment optimization schemes (Wang & Chen, 2011). However, most current research lacks consideration of drivers' visual perception.

## 2.3 | CycleGAN

CycleGAN is an unpaired image-to-image translation algorithm, which was first proposed by Zhu et al. (2017). It can transfer the style of one set of images onto another style to create new images without any paired training examples (Gatys et al., 2016). The object of image style transfer can be abstract styles or instance objects (Isola et al., 2017).

CycleGAN has demonstrated remarkable performance in various environment image translation and generation tasks. For example, Karlsson and Welander (2018) employed CycleGAN to generate visually realistic street view images with various resolutions, lighting conditions, and weather scenarios. Besides, another study used CycleGAN to translate road environment images from night to day, to increase background brightness and improve nighttime vehicle detection accuracy (Shao et al., 2020). In the current research, CycleGAN-based environment




**TABLE 2** Summary of the facility environment semantics affecting drivers' speed selection on rural roads.

Study	Analyzed facility environment semantics	Comprehensive analysis	Results		Drivers' visual perception
			Property	Specific findings	
Goldenbeld and van Schagen (2007)	Roadside buildings, trees, vegetation	No	Quantitative	Roadside buildings and trees can reduce drivers' preferred speeds by about 5 km/h	No
Broughton et al. (2009)	Roadside surrounding	No	Qualitative	Drivers tend to speed on empty roads	No
Cruzado and Donnell (2010)	Warning sign, number of warning signs	Yes	Qualitative	Warning signs can reduce operation speeds, and more signs further enhance their impact	No
Bella (2013)	Roadside configuration	No	Qualitative	No guardrail, standard guardrail and red-and-white guardrail have little effect on operation speeds	No
Antonson et al. (2014)	Trees, buildings, barriers, road signs, shoulders, landscapes	Yes	Qualitative	Trees, buildings, and barriers are more likely to reduce driving speeds	No
Montella et al. (2015)	Warning signs, perceptual measures, and transverse rumble strips	No	Quantitative	Warning signs, perceptual countermeasures, and transverse rumble strips can reduce average speeds by about 3, 12, and 6 km/h, respectively	No
Cox et al. (2017)	Road signs, traffic lights, tree	Yes	Qualitative	Trees are more likely to reduce driving speeds	No
Yu et al. (2019)	Landscapes, barriers, obstacles, traffic signs	Yes	Qualitative	Abundant landscapes, obstacles and continuous barriers significantly reduce the speeding likelihood	Yes
Vignali et al. (2019)	Roadwork signs	No	Quantitative	Roadwork signs can reduce the average driving speed by about 20 km/h	Yes
Ambros et al. (2020)	Median barrier	No	Qualitative	Speeding increases with the progression from no barrier to solid barrier to cable barrier	No
Qin et al. (2020)	Traffic sign, roadside landscape, pavement markings, protection facilities	No	Quantitative	High-density roadside greenery can reduce driving speeds by more than 25 km/h	Yes

image generation and translation technologies are limited to alterations in images' visual representation effect (i.e., the abstract style of images) and do not have much practical impact on environment optimization in engineering applications.

After the facility environment optimization scheme is determined, optimizing the facility environment from drivers' visual perception can be regarded as transforming the existing unsuitable facility environment images into corresponding optimized images by adjusting the facility environment semantics (i.e., instance objects). CycleGAN-based image translation and generation tech-

nologies can automatically learn mappings between different domains without the need for extensive manual data labeling, which could significantly reduce the human effort required during the optimization process (Almahairi et al., 2018). However, there is currently no related research.

Given the above, there exists a gap in conducting a comprehensive and quantitative analysis of how various facility environment semantics influence drivers' speed selection from drivers' visual perception. Besides, the current facility environment optimization is unable to consider the original facility environment characteristics and

offers limited optimization methods. It heavily relies on human work and expert experiences, lacking prompt verification of the optimization effect. Therefore, this study proposes an intelligent optimization method, which could optimize the facility environment on rural roads from drivers' visual perception. In this study, a visual road schema model is established to quantitatively quantify the facility environment from drivers' visual perception. Furthermore, an automated approach for determining the optimization scheme is proposed using self-explaining theory, which comprises two steps: assessing the applicability of the original facility environment semantics and proposing optimization principles. After that, this study puts forward a CycleGAN-based optimization model to intelligently optimize the original facility environments according to the optimization schemes, and a random forest model is built to verify the optimization effect by predicting the operation speeds of the optimized facility environments. The main contributions of this paper are as follows:

First, a visual road schema model that quantitatively quantifies the semantic composition of facility environments and measures the speed revision ability of these semantics from drivers' visual perception.

Second, an automated method for determining facility environment optimization schemes:

1. The proposed optimization schemes consider the original characteristics of facility environments (i.e., semantic composition and speed revision ability of each semantic), ensuring the most effective treatments for the original facility environments.
2. Various optimization schemes may be proposed, involving four categories of semantics (i.e., visual lane markings, visual pulses, roadside protections, and landscapes) and their combinations.

Third, an efficient and automated method to realize the optimization scheme from drivers' visual perception (i.e., transfer the original visual image of the facility environment into an optimized version directly), with the ability to promptly verify the optimization effects.

### 3 | FRAMEWORK

The framework of this study is proposed in Figure 1, which briefly illustrates the intelligent optimization method for the facility environment on rural roads.

First, as shown in Figure 1a, facility environments where operation speeds exceed the speed limit are screened out and are quantitatively quantified from drivers' visual perception with the visual road schema model. Specifically,

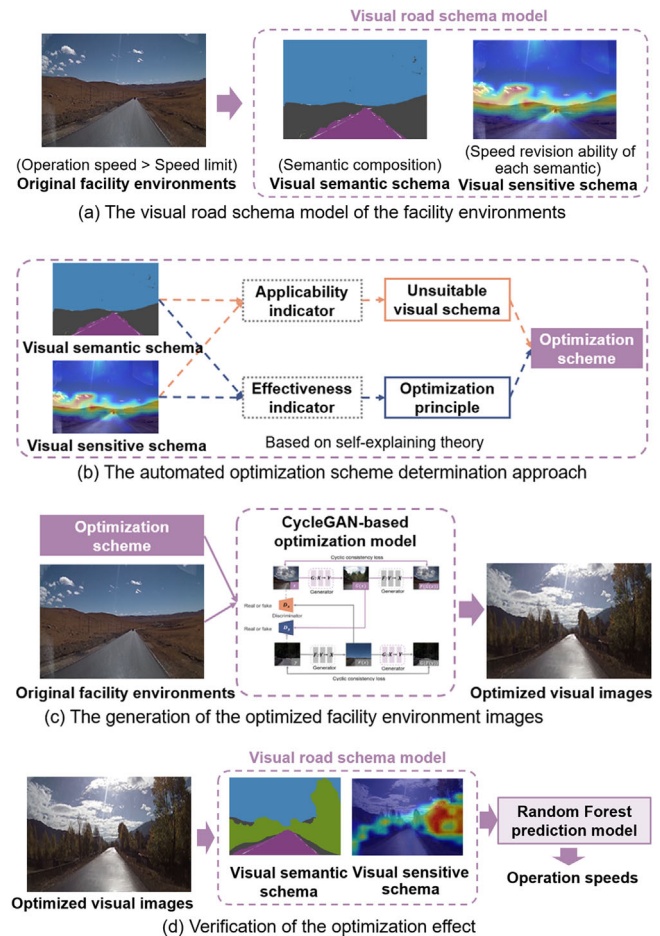


FIGURE 1 The intelligent optimization method.

the visual semantic schema and visual sensitive schema are extracted, which reflect the semantic composition of facility environments and the speed revision ability of each semantic, respectively.

Then, as illustrated in Figure 1b, the optimization schemes for the original facility environments are automatically determined with the applicability and effectiveness indicators. These two indicators are developed through statistical analysis and align with the self-explaining theory. The applicability indicator is used to judge whether the visual semantic and sensitive schemas of the original facility environments are suitable. The effectiveness indicator helps to determine how the unsuitable visual semantic and sensitive schemas should be optimized.

After that, as indicated in Figure 1c, to realize the optimization scheme, the CycleGAN-based optimization model is employed to automatically optimize the original facility environments into suitable ones from drivers' visual perception directly (i.e., transfer the original visual images of the facility environment into an optimized version).



At last, as presented in Figure 1d, the optimized facility environments are quantified using the visual road schema model, and a random forest model is employed to verify the optimization effect by predicting the operation speeds of the optimized facility environments with this model. If the predicted operation speeds are below the speed limit, the optimization is completed. If not, the optimization step should be repeated until the predicted operation speeds align with the speed limit. More details of this study are provided in the following sections.

## 4 | NATURALISTIC DRIVING EXPERIMENT

A series of naturalistic driving experiments were carried out on two-way two-lane rural roads in five provinces across China (including Tibet, Anhui, Shandong, Jiangxi, and Zhejiang), with a total travel distance of more than 50,000 km. Road sections used in this study consist of mountain roads, township roads, and other categories containing varied roadside landscapes and road facilities. Each road section had a clearly defined speed limit. All road sections had relatively low traffic volume, which imposed little influence on driving behavior. The experiment involved a total of 42 drivers, comprising 33 males and nine females. Participants' ages ranged from 23 to 50 years, with a mean age of 32.9 years and a standard deviation (SD) of 7.1 years. All participants were local residents who were familiar with the road environment and had a minimum of 3 years of driving experience, with an average of 11.3 years, a SD of 5.8 years, and a range from 3 to 22 years.

The data collected from each driver included at least driving data of 1000 km. These experiments used a driving recorder (GARMIN GDR35), a Global Positioning System (GPS) locator, and a three-axis acceleration sensor to obtain driving videos and kinematic vehicle information. The driving recorder could precisely align GPS positions with driving video information and was positioned within the drivers' line of vision to capture the facility environment perceived by drivers. A sampling rate of 1 Hz was used. A total of 3502 sets of valid data were obtained in this study after screening and processing. Each dataset included an RGB road section figure from the drivers' visual point of view, the geographic coordinate, and the operation speed of the facility environment (i.e., the 85th percentile of all drivers' speeds).

In this study, speeding is defined as operation speeds exceeding the speed limits, which indicates that most drivers tend to overspeed in these facility environments (Hou et al., 2020). Based on this criterion, there are 1190 such road sections with high tendencies of speeding, tak-

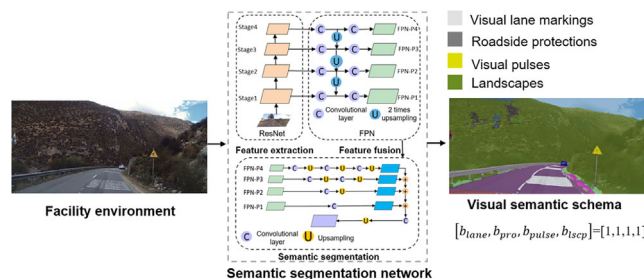


FIGURE 2 The visual semantic schema.

ing about 34% of the total data. Other road sections are considered with low tendencies of speeding.

## 5 | THE VISUAL ROAD SCHEMA MODEL

A visual road schema model is established to quantitatively quantify drivers' visual perception of the facility environment during driving, including the visual semantic schema and visual sensitive schema.

### 5.1 | The visual semantic schema

As demonstrated in Figure 2, the visual semantic schema demonstrates the semantic composition of rural roads perceived by drivers.

A modified semantic segmentation network composed of feature extraction, feature fusion, and semantic segmentation is adopted to establish the visual semantic schema. The features of objects in the original image are first retained through the feature extraction module (i.e., a residual neural network [ResNet]). Then, they are input into the feature pyramid network for feature fusion. Finally, the semantic segmentation branch is used to identify various semantics of the facility environment. Pixels belonging to the same semantic are labeled with a specific color. More information on the semantic segmentation network is available from our previous study (Chen et al., 2021). Semantics are further divided into four categories: visual lane markings (e.g., dividing lines, edge lines, etc.), roadside protections, visual pulses (e.g., traffic signs, colored pavements, advertising boards, etc.), and landscapes, represented in the visual semantic schema by light gray (RGB: 255, 255, 255), gray (RGB: 125, 125, 125), yellow (220, 220, 0), and green (107, 142, 35), respectively.

The visual semantic schema can be denoted by a vector  $[b_{lane}, b_{pro}, b_{pulse}, b_{lscp}]$ . Elements in the vector describe the four semantic categories' presence, each of which takes a value of 0 or 1. If a semantic category is included in the



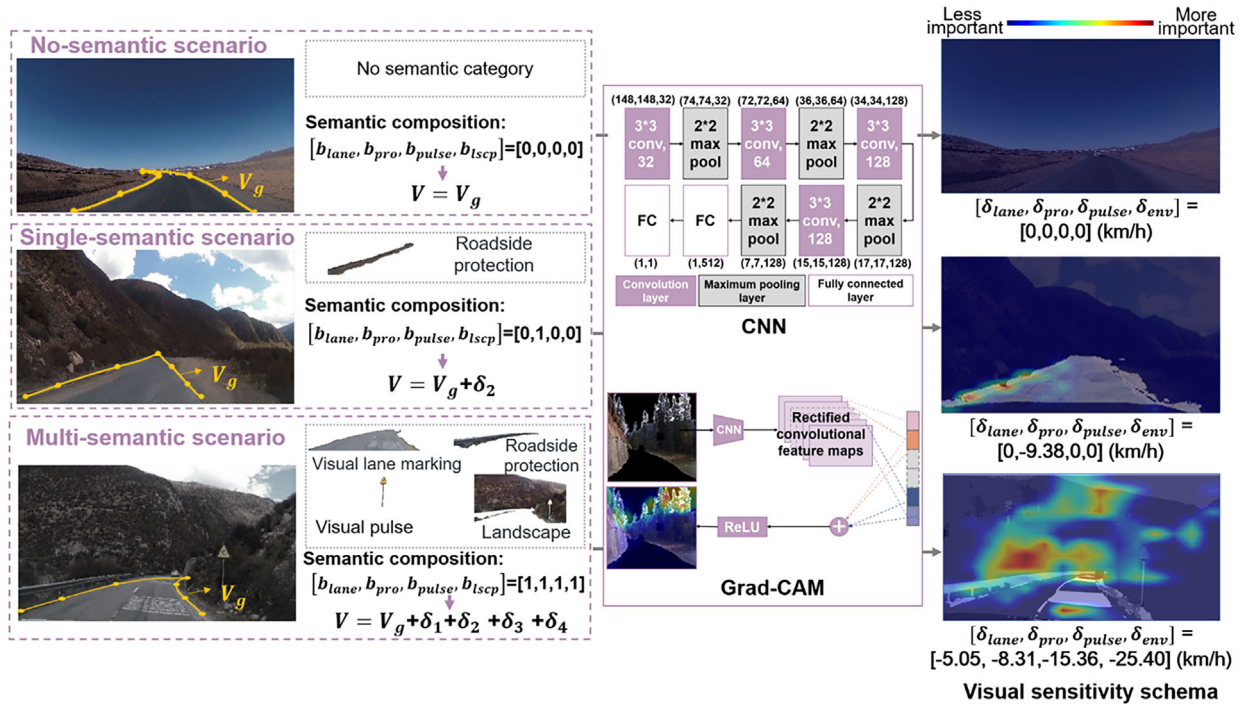


FIGURE 3 The visual sensitive schema.

facility environment, the corresponding element value is labeled as 1; otherwise, 0.

## 5.2 | The visual sensitive schema

As illustrated in Figure 3, the visual sensitive schema is used to represent the speed revision ability of each semantic.

According to our previous study (Qin et al., 2020), the visual road geometry determines drivers' basic speeds, and the facility environment has an additional revision ability. In this study, the visual sensitive schema is a quantification of the revision ability. As shown in Equation (1), the actual operation speed  $V$  depends on the basic speed  $V_g$  and the revised component  $\delta$  of the speed.

$$V = V_g + \delta \quad (1)$$

$$\delta = \sum_i^n \delta_i \quad (2)$$

In Equation (2),  $\delta$  is the total value of the revised component,  $\delta_i$  represents revised components of speeds of different semantic categories,  $i \in N^+$ , indicating the visual road marking, roadside protection, visual pulse, and landscape.  $\delta_i < 0$  means that the semantic has an inhibitory effect on the speed of drivers, while  $\delta_i > 0$  represents a promoting influence.

According to the number of semantic categories in scenarios, the facility environment is divided into three types: no-semantic scenario, single-semantic scenario, and multi-semantic scenario.

In the no-semantic scenario, the operation speed is only affected by the visual road geometry, namely,  $V = V_g$  and  $\delta = 0$ . Based on our previous research (Yu et al., 2019), the CatMull-Rom spline curve could fit the visual road geometry well, and the shape parameters of the CatMull-Rom spline curve (i.e., the visual curve length and curvature of adjacent control points) are closely related to basic speeds. Therefore, the random forest model is employed to predict the basic speed  $V_g$  through these shape parameters. The optimal hyperparameters for the random forest model are determined through cross-validation. Specifically, the optimal parameters for the model are found to be 192 trees, a maximum tree depth of 6, and eight features considered at each split. The model achieves a mean absolute error of 1.29 km/h and an out-of-bag (OOB)  $R^2$  of 0.96 on the testing set, indicating a good regression performance.

In the single-semantic scenario, there is only one category of semantics (i.e.,  $\delta = \delta_i$ ), and  $\delta$  can be calculated by taking the difference between  $V$  and  $V_g$ .

In the multi-semantic scenario, there are two or more categories of semantics, and the speed revision ability of different semantics should be compared and analyzed. The convolutional neural network (CNN) and the Gradient-weighted Class Activation Mapping (Grad-CAM) technique are used to calculate the relative importance



ratio of various semantic categories and allocate the total value of the revised speeds (i.e.,  $\delta$ ) based on this ratio. CNN is a class of deep learning algorithms containing convolutional computation, which is widely used in image understanding and calculation (Alzubaidi et al., 2021). Grad-CAM is a class-discriminative localization technique for CNN-based models, which can highlight the regions in an image that are important for the model's prediction (Jingjing Guo et al., 2021).

The visual sensitive schema could be represented by a vector  $[\delta_{lane}, \delta_{pro}, \delta_{pulse}, \delta_{lscp}]$ . Elements in the vector describe the revised speeds of the visual road marking, roadside protection, visual pulse, and landscape. Figure 3 shows some examples of the visual sensitive schema in no-semantic, single-semantic, and multi-semantic scenarios.

## 6 | THE AUTOMATED OPTIMIZATION SCHEME DETERMINATION APPROACH

To determine the optimization scheme for the original facility environment, a self-explaining analysis of the visual road schema is conducted, including the applicability and effectiveness analyses. The applicability analysis evaluates whether the original visual semantic and sensitive schemas are suitable for rural roads, while the effectiveness analysis helps determine how to optimize the unsuitable visual semantic and sensitive schemas. These analyses are developed with effectiveness and applicability indicators for visual semantic and sensitive schemas proposed in this study based on statistical methods. Sections 5.1 and 5.2 describe the process for determining these indicators for visual semantic and sensitive schemas, respectively, as well as how to apply them to automatically determine the optimization scheme for the facility environment.

### 6.1 | The effectiveness and applicability indicators for the visual semantic schema

When facility environments look similar, they are categorized as the same from drivers' visual perception, and road users generate similar driving speeds (Theeuwes, 2021). Therefore, the effectiveness indicator for the visual semantic schema is proposed by exploring the influence of different semantic combinations of the facility environment on operation speeds. Besides, this study summarizes the visual semantic schema suitable for rural roads (i.e., the applicability indicator for the visual semantic schema), by comparing the semantic composition differences between road sections with high and low tendencies of speeding.

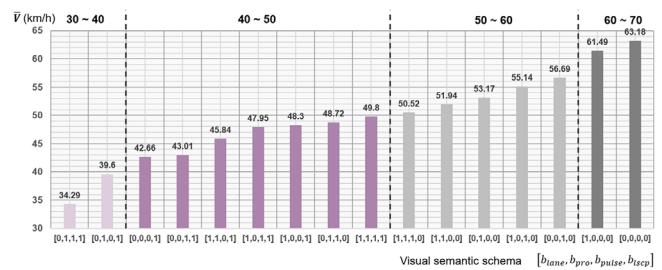


FIGURE 4 The effectiveness indicator for the visual semantic schema: the visual semantic schema with different semantic combinations and their corresponding operation speed intervals.

The facility environment on rural roads includes four semantics, namely, the visual lane marking, roadside protection, visual pulse, and landscape, and there are 16 groups of visual semantic schemas with different semantic combinations. Figure A1 in the Appendix presents the mean and SD of operation speeds of each visual semantic schema.

#### 6.1.1 | The effectiveness indicator

Before summarizing the effectiveness indicator for the visual semantic schema, the analysis of variance (ANOVA) is conducted for the operation speed samples collected under 16 groups of visual semantic schemas to verify whether the visual semantic schema has a significant effect on operation speeds. ANOVA tests whether the differences between groups are beyond what can be explained by random error alone (Kim, 2017). The results are summarized in Table 3. All the samples in each group meet the applicable conditions of ANOVA. The data are normally distributed, and homoscedasticity is guaranteed (Levene's Test,  $p < 0.05$ ). The result of ANOVA shows that the impacts of different semantic combinations on operation speeds are significantly distinct ( $F(15, 3486) = 126.156$ ,  $p < 0.05$ ). In other words, it is statistically valid to alter drivers' road category cognition by changing the visual semantic schema.

Then, the corresponding speed intervals for the visual semantic schema with different semantic combinations are summarized in Figure 4, namely, the effectiveness indicator for the visual semantic schema. According to the speed limit of the road section, the appropriate visual semantic schema could be selected as the optimization target with this indicator.

#### 6.1.2 | The applicability indicator

To explore the applicability indicator for the visual semantic schema, the proportion of road sections with



TABLE 3 Results of ANOVA under different semantic combinations of visual semantic schemas.

Levene's test					
Levene statistics	DF1	DF2	p-value		
6.226	15	3486	<0.001		
Tests of between-subjects effects					
Dependent variable: Operation speeds					
	Type III SS	DF	MS	F	p-value
Modified model	291,019.88	15	19,401.33	126.156	<0.001
Intercept	3,032,710.02	1	3,032,710.02	19,720.100	<0.001
Semantics	291,019.88	15	19,401.33	126.156	<0.001
Error	536,104.14	3486	153.79		
Sum	17,051,531.00	3502			

Abbreviation: ANOVA, analysis of variance.

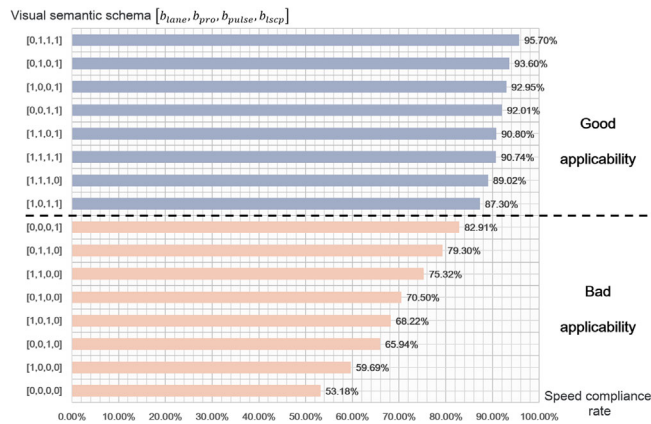


FIGURE 5 The applicability indicator for the visual semantic schema: the speed compliance rate for each visual semantic schema.

high tendencies of speeding among all road sections (i.e., speed compliance rate) of each visual semantic schema is calculated, and those with a probability exceeding 85% are considered to have good applicability on rural roads as demonstrated in Figure 5. It could be seen that visual semantic schemas with fewer semantics tend to show poorer applicability. In contrast, visual semantic schemas with rich roadside landscapes and road facilities demonstrate greater applicability. Among all semantics, the landscape plays an essential role in improving the applicability of the facility environment on rural roads. Almost all visual semantic schemas containing landscapes are applicable on rural roads, which is consistent with the current research (Van Treese et al., 2017).

The applicability indicator for the visual semantic schema can be summarized as follows: If the visual semantic schema of the facility environments falls within [0,1,1,1], [0,1,0,1], [1,0,0,1], [0,0,1,1], [1,1,0,1], [1,1,1,1], [1,1,1,0], or [1,0,1,1], they are considered good applicability on rural roads; otherwise, they are considered bad applicability. To

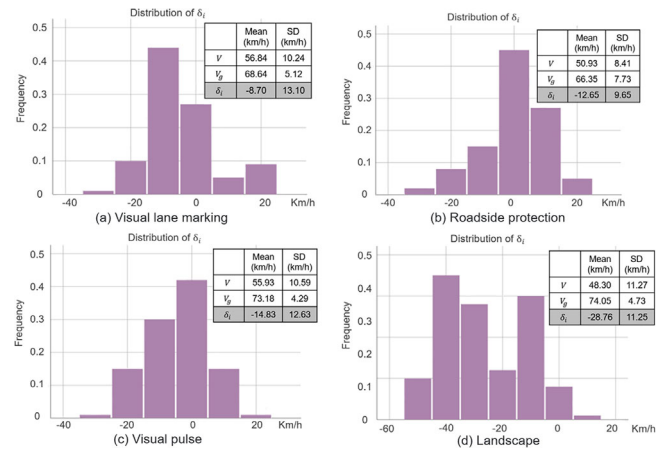


FIGURE 6 The distribution of drivers' revised speeds in each single-semantic scenario.

optimize the visual semantic schema with bad applicability, one or more semantics could be modified comprehensively considering the current semantic composition and engineering quantity.

## 6.2 | The effectiveness and applicability indicators for the visual sensitive schema

### 6.2.1 | The effectiveness indicator

The visual sensitive schema reflects the speed revision ability of specific semantics on operation speeds. In single-semantic scenarios with different semantics, the distributions of operation speeds  $V$ , basic speeds  $V_g$ , and revised speeds  $\delta_i$  are calculated. As illustrated in Figure 6, all mean values of  $V$  are lower than those of  $V_g$ , which indicates that all semantics generally have an inhibiting effect on operation speeds.

To determine the effectiveness indicator for the visual sensitive schema, various levels are divided according to





**TABLE 4** The effectiveness indicator for the visual sensitive schema: Speed revision ability level of each semantic.

	Level 1 (km/h)	Level 2 (km/h)	Level 3 (km/h)
Visual lane marking	0	−10	
Roadside protection	0	−15	
Visual pulse	0	−15	
Landscape	0	−15	−40

the speed revision ability of different semantics. As shown in Figure 6a, the revised speed caused by visual lane marking is the lowest, with an average of  $-8.70$  km/h. Thus, this semantic is split into two levels: (1) no visual lane marking,  $\delta_i = 0$ ; (2) the visual lane marking exists in the facility environment,  $\delta_i \approx -10$  km/h. In addition, the mean values of the revised speed of visual pulses and roadside protections are  $-12.65$  and  $-14.83$  km/h (see Figure 6b,c), respectively. Similar to the visual lane marking, these two semantics are also divided into two levels according to the speed revision ability ( $\delta_i = 0$  or  $\delta_i \approx -15$  km/h).

As demonstrated in Figure 6d, the revised speed caused by the landscape is the largest and has the largest range, distributed from  $-50$  to  $10$  km/h, with two humps at  $-40$  and  $-15$  km/h. The appearance of the two humps indicates that the landscape could not use the same classification method that only is divided into two levels, as with the other three semantics. Based on the psychological investigation, it is found that drivers subconsciously assume that roads surrounded by abundant plants or buildings are access roads rather than arterial highways and reduce their speed accordingly (Charlton & Starkey, 2017). In addition, the density of the roadside landscape could to some extent, influence driving behavior (Van Treese et al., 2017). Compared to the empty landscape, dense vegetation and housing help drivers choose appropriate driving speeds and appear to enhance the roadway's safety performance (H. Liu, 2013). Therefore, it is necessary to distinguish the speed revision effects of the landscape with different densities. As a result, the effectiveness of the landscape could be divided into three levels according to the speed revision ability: (1) no landscape,  $\delta_i = 0$ ; (2) low-density landscapes,  $\delta_i \approx -15$  km/h; (3) landscapes with dense vegetation and housing,  $\delta_i \approx -40$  km/h.

Modifying the facility environment to adjust operation speeds could be considered as a migration of speed revision ability levels with different semantics. Table 4 summarizes the speed revision ability level of each semantic (i.e., the effectiveness indicator for the visual sensitive schema), which could provide guidance for proposing optimization schema by offering a rough estimate of the optimization effect.

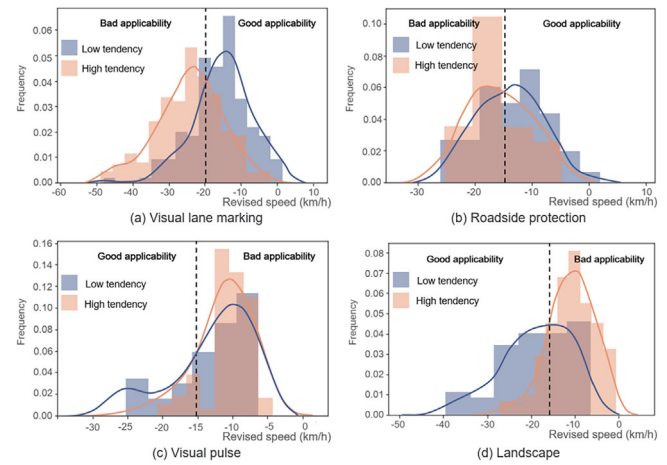


**FIGURE 7** Distribution diagrams of revised speeds on road sections with high and low tendencies of speeding.

## 6.2.2 | The applicability indicator

Then, this study explores the applicability indicator for the visual sensitive schema. The probability distributions of revised speeds of different semantics on road sections with high and low tendencies of speeding are counted as shown in Table 5 and Figure 7. Significance testing for differences in revised speeds of different semantics between these road sections with high and low tendencies of speeding is examined using the Kruskal–Wallis test (MacFarland & Yates, 2016). The results in Table 5 show significant differences in revised speeds of each semantic on these road sections ( $p < 0.001$ ).

In addition, probability distributions of revised speeds are fitted by kernel density, and the threshold of revised speeds with good applicability is determined according to the intersection point of two kernel density functions in each semantic (see Table 5 and Figure 7). For the visual lane marking, if  $\delta_i > -20$  km/h, there is a higher tendency of speeding. Similarly, for the roadside protection, if  $\delta_i > -15$  km/h, there is a lower tendency for speeding in road sections. As for the visual pulse, road sections exhibit a lower tendency for speeding when  $\delta_i \leftarrow 15$  km/h. For the landscape, road sections demonstrate a lower speeding tendency if  $\delta_i \leftarrow 15$  km/h.

In conclusion, the ranges of applicability of revised speeds for the visual lane marking, roadside protection, visual pulse, and landscape of rural roads (i.e., the applicability indicator for the visual sensitive schema) are set as  $[-20$  km/h,  $0$  km/h],  $[-15$  km/h,  $0$  km/h],  $[-30$  km/h,  $-15$  km/h], and  $[-40$  km/h,  $-15$  km/h], respectively. When the revised speeds of semantics are within the ranges, it is more likely to facilitate appropriate operation speeds.



**TABLE 5** The applicability indicator for the visual sensitive schema: Distributions of revised speeds on road sections with high and low tendencies of speeding and the result of significance testing.

	High tendency		Low tendency		p-value	Good applicability
	Mean (km/h)	SD (km/h)	Mean (km/h)	SD (km/h)		
Visual lane marking	-3.83	8.38	-3.12	5.68	<0.001	[-20 km/h, 0 km/h]
Roadside protection	-3.83	6.98	-0.38	2.44	<0.001	[-15 km/h, 0 km/h]
Visual pulse	-1.12	3.89	-0.59	2.67	<0.001	[-30 km/h, -15 km/h]
Landscapes	-8.51	9.93	-19.84	12.35	<0.001	[-40 km/h, -15 km/h]

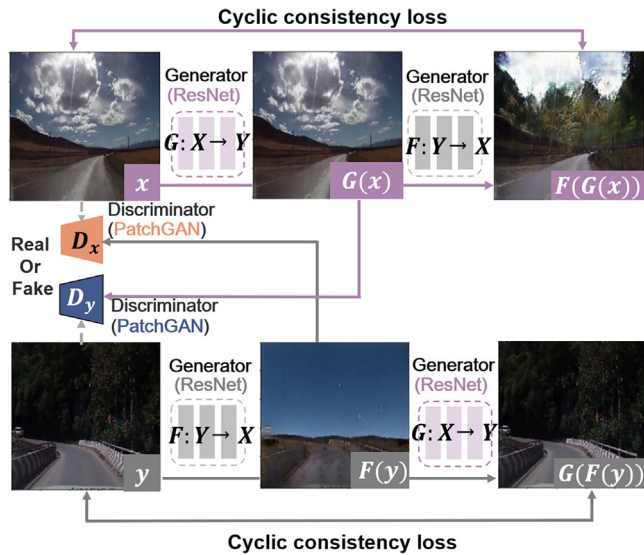


**FIGURE 8** The Cycle-consistent generative adversarial network (CycleGAN) network structure.

## 7 | THE GENERATION OF THE OPTIMIZED FACILITY ENVIRONMENT IMAGES

In this study, CycleGAN is used to automatically generate optimized facility environment images according to the optimization scheme.

The CycleGAN consists of two mirror-symmetric Generative Adversarial Network (GAN) models, and the network structure is shown in Figure 8. It aims to build mapping functions between two categories,  $X$  and  $Y$  (i.e.,  $G: X \rightarrow Y$  and  $F: Y \rightarrow X$ ). The network contains two generators ( $G$  and  $F$ ) and two discriminators ( $D_x$  and  $D_y$ ). The generator  $G$  could convert image  $x$  in category  $X$  to image  $G(x)$  under category  $Y$ , and generator  $F$  is responsible for converting image  $y$  under category  $Y$  to image  $F(y)$  under category  $X$ . Discriminators  $D_x$  and  $D_y$  are used to identify the authenticity of  $X$  and  $Y$  category images, respectively. In the process of model training, the generators' goal is to improve the accuracy of the generated image as much as possible to "fool" the discriminators, while the discriminators aim to recognize the fake image generated by the

generator. For example, for the mapping function  $G: X \rightarrow Y$ , generator  $G$  generates images  $G_x$  similar to images from category  $Y$ , and  $D_y$  is devoted to distinguishing between  $G_x$  and real samples  $y$ . The same process applies to the other mapping function  $F: Y \rightarrow X$ . Therefore, the CycleGAN network consists of two basic adversarial losses, as below.

$$L_{GAN(G,D_Y,X,Y)} = \mathbb{E}_{y \sim p_{data}(y)} [\log D_Y(y)] + \mathbb{E}_{x \sim p_{data}(x)} [\log(1 - D_Y(G(x)))] \quad (3)$$

$$L_{GAN(F,D_X,Y,X)} = \mathbb{E}_{x \sim p_{data}(x)} [\log D_X(x)] + \mathbb{E}_{y \sim p_{data}(y)} [\log(1 - D_X(F(y)))] \quad (4)$$

where  $L_{GAN(G,D_Y,X,Y)}$  and  $L_{GAN(F,D_X,Y,X)}$  indicate adversarial losses;  $y \sim p_{data}(y)$  and  $x \sim p_{data}(x)$  refer to the training examples  $x$  and  $y$ , respectively, which are sampled from two different and unknown distributions,  $p_{data}(x)$  and  $p_{data}(y)$ ;  $\mathbb{E}$  stands for expectation operation;  $\log D_Y(y)$  and  $\log D_X(x)$  denote the logarithm of the probability that the discriminator correctly classified real samples as real, while  $\log(1 - D_Y(G(x)))$  and  $\log(1 - D_X(F(y)))$  denote the logarithm of the probability that the discriminator incorrectly classifies generated samples as real.

Driven by a large sample, the generated image may be mapped to any image in the target domain. Therefore, the cyclic consistency loss is introduced to constrain consistency between fake images (Kwak & Lee, 2020). As shown in Figure 8, after the original image  $x$  is translated into  $G(x)$  by generator  $G$ , the generated image is reconstructed into the image  $F(G(x))$  by generator  $F$ , which should be as similar as possible to  $x$  (i.e.,  $F(G(x)) \approx x$ ). In addition,  $G(F(x))$  should also be as similar to  $y$  as possible.

The cyclic consistency loss  $L_{cyc(G,F)}$  can be expressed as follows:

$$L_{cyc(G,F)} = \mathbb{E}_{x \sim p_{data}(x)} [\|F(G(x)) - x\|_1] + \mathbb{E}_{y \sim p_{data}(y)} [\|G(F(y)) - y\|_1] \quad (5)$$

where  $\|F(G(x)) - x\|_1$  and  $\|G(F(y)) - y\|_1$  refer to the L1-norm distance between  $F(G(x))$  and  $x$  and  $G(F(y))$  and  $y$ , respectively.





The  $\lambda$  is defined as the relative importance coefficient of cyclic consistency and the comprehensive loss function of the CycleGAN network  $L(G, F, D_X, D_Y)$  is as shown below:

$$L(G, F, D_X, D_Y) = L_{GAN(G, D_Y, X, Y)} + L_{GAN(G, D_X, Y, X)} + \lambda L_{cyc(G, F)} \quad (6)$$

As demonstrated in Figure 8, to ensure the efficiency and quality of image translation, this study employs the deep residual CNN (ResNet) as the generator and the Markovian discriminator (PatchGAN) as the discriminator. ResNet is a deep neural network architecture that incorporates residual blocks and it is a common choice for CycleGAN generators due to its ability to produce realistic images with limited training data (K. He et al., 2016). PatchGAN employs patch-level discrimination by dividing the input image into image patches, resulting in a discriminator network with fewer parameters and increased efficiency (Isola et al., 2017). This combination of the generator and discriminator has been proven to have a good image-generation effect and strong network robustness (Zhu et al., 2017).

As mentioned in Section 5.2, each semantic is split into two or three levels according to speed revision ability. A CycleGAN model is established for each level pair as demonstrated in Figure 9. The visual lane marking is divided into two levels based on speed revision ability, and its presence or absence is considered as two objects for image translation (refer to Figure 9a). Similarly, roadside protection and visual pulse have the same idea of image translation as shown in Figure 9b,c. The landscape contains three levels, and the CycleGAN network regards landscape density as the classification standard. The landscape with different levels of speed revision ability could be transferred from one to another (see Figure 9d,e,f).

In this study, CycleGAN models are implemented using the PyTorch deep learning framework. Adam is selected as the network optimizer, and the initial learning rate of the generator  $G$  and discriminator  $D$  is set at 0.0002. Adam is an optimization algorithm based on adaptive estimates of lower-order moments, which is commonly employed for minimizing the loss between the generators and discriminators because of its ease of implementation, good convergence properties, computational efficiency, and low memory requirements (Kingma & Ba, 2014). The maximum iteration number of training is set to 100, and the size of each batch is 1. After training about 80 epochs, the model generation effect tends to be stable.

## 8 | VERIFICATION OF THE OPTIMIZATION EFFECT

To evaluate the optimization effect, the random forest model is utilized to predict the operation speeds of the optimized facility environment based on the visual semantic schema and visual sensitive schema. The optimization is considered successful if the predicted operation speed is within the speed limit.

The random forest algorithm is an ensemble learning approach that predicts outcomes by combing the bootstrapped aggregation of several regression trees (Zhong et al., 2023). The random forest algorithm has high accuracy, and it can efficiently handle massive datasets without dimensionality reduction (Y. Xu et al., 2021). In addition, it does well in handling data heterogeneity and complex data structures (Wager & Athey, 2018). In this model, there are nine input variables, including the basic speed  $V_g$ , the visual semantic schema  $[b_{lane}, b_{pro}, b_{pulse}, b_{lscp}]$ , and the visual sensitive schema  $[\delta_{lane}, \delta_{pro}, \delta_{pulse}, \delta_{lscp}]$ , while the operation speed  $V$  is the dependent variable. The model is trained and tested using the Scikit-learn package in Python.

A total of 3502 images are used in establishing the random forest model. About 85% of them are randomly selected as the testing set, and the remaining 15% as the testing set. There are several self-defined parameters, including the number of trees ( $n_{trees}$ ), the maximum tree depth ( $d_{max}$ ) and the number of features considered at each split ( $n_{features}$ ). To determine the optimal combination of these parameters, the grid search and cross-validation are employed.

When  $n_{features} = 5$ ,  $d_{max} = 9$ ,  $n_{trees} = 189$ , the model has the best performance with the OOB  $R^2$  of 0.90 and the mean squared error of 0.58 km/h. Figure 10 illustrates that the random forest model performs well in predicting operation speeds.

## 9 | CASE STUDY

Several continuous road sections in Anhui Province, China, are selected to verify the intelligent optimization method for the facility environment on rural roads proposed in this study. The speed limit is 50 km/h on these road sections. As shown in Figure 11a, operation speeds on these road sections are much higher than the speed limit, making them urgently in need of optimization. Road Section 5, with an operation speed of 65.42 km/h, is taken as an example to describe the whole optimization process.

First, the facility environment of the road section 5 is quantitatively quantified with the visual road schema

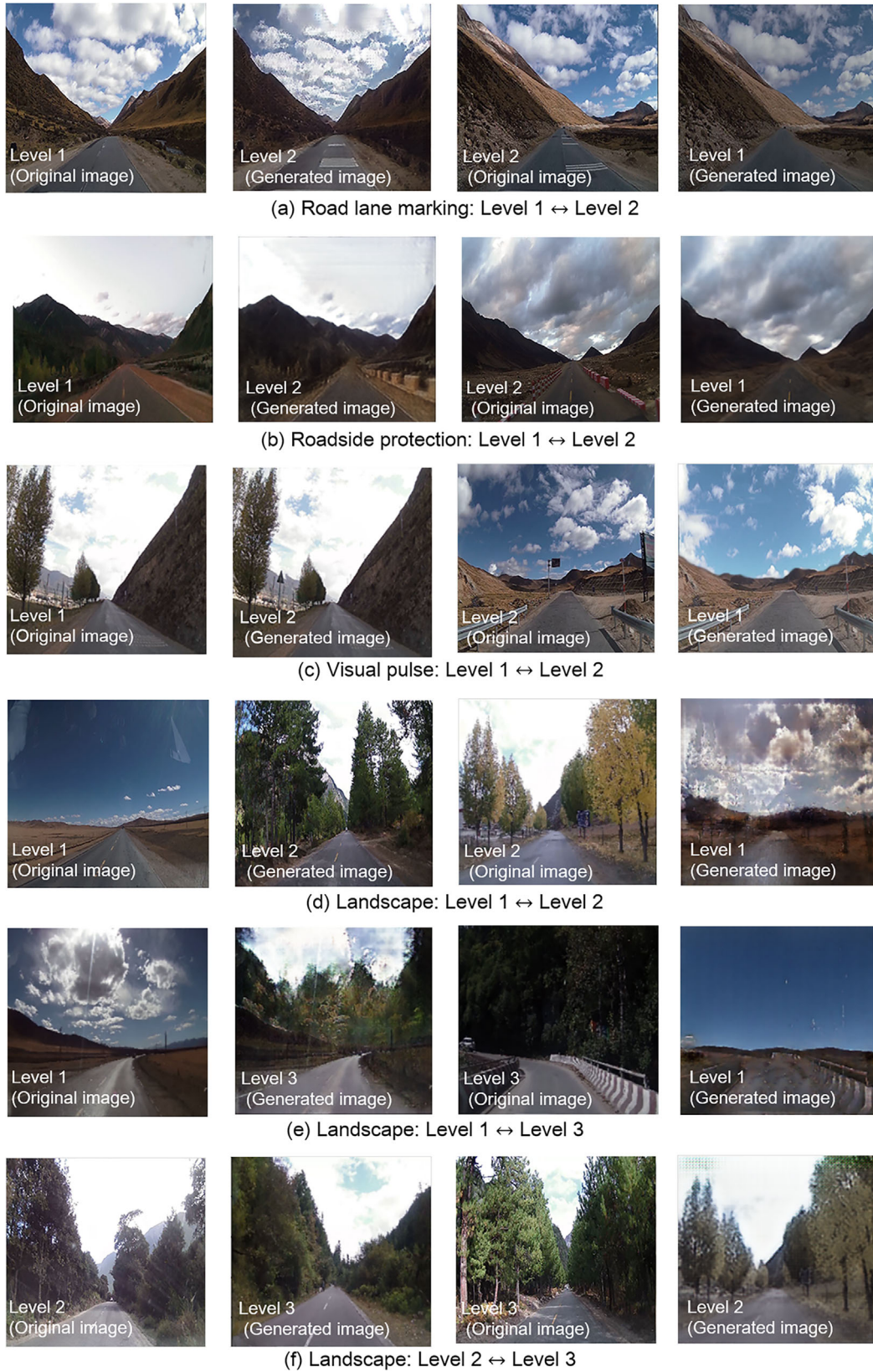


FIGURE 9 The effect of the optimization model based on CycleGAN.



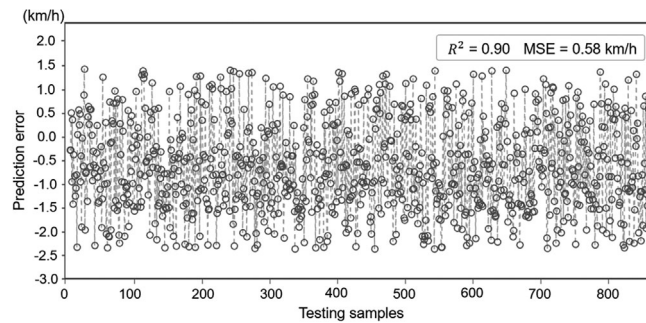


FIGURE 10 The prediction result of the random forest model.

model described in Section 4. Figure 11b demonstrates the visual image along with the visual semantic and sensitive schemas of road section 5. The driver's basic speed on this road section is calculated as 71.79 km/h. According to the visual semantic schema, the facility environment on this road section contains only the visual lane marking, which could be represented by the vector  $[1,0,0,0]$ . Accordingly, the revised speed generated by the visual lane marking is calculated as  $-6.37$  km/h and the visual sensitive schema vector of this road section is  $[-6.37,0,0,0]$ .

Then, the optimization scheme for the original facility environment of the road section 5 is determined with the applicability and effectiveness indicators. Referring to the applicability indicator for the visual semantic schema in Figure 5, the current visual semantic schema of the road section  $[1,0,0,0]$  is unsuitable for rural roads. Both sides of the road are sand and stones, and the surrounding landscape is relatively empty, which reduces driver attentiveness and leads to the cognitive deviation of the road category (Ma et al., 2018). Drivers may temporarily forget that they are driving on a low-category rural road, which results in high driving speeds (Qin et al., 2020). In accordance with the applicability indicator for the visual sensitive schema in Table 5, the revised speed of the existing visual lane marking is suitable and does not need to be modified. This intelligent optimization method has gained recognition and adoption by the local government and the Anhui Provincial Institute of Transportation Planning and Design. Since the speed limit of this road section is 50 km/h, based on the effectiveness indicator for the visual semantic schema (see Figure 4), the semantic combination of  $[1,1,0,1]$ ,  $[1,0,1,1]$ ,  $[1,0,0,1]$ , and  $[1,1,1,1]$ , which contain the visual lane marking, could effectively guide the operation speed of 40–50 km/h. Among them,  $[1,0,0,1]$  has the highest speed compliance rate and is the best optimization scheme, according to the rank in Figure 5. The operation speed on this road section needs to be reduced by approximately 15 km/h to satisfy the speed limit requirement. Therefore, according to the effectiveness indicator for the visual sensitive schema (see Table 4), this study transfers

the speed revision ability of the landscape from Level 1 to Level 2 to achieve the target operation speed.

After that, the trained CycleGAN model is used to implement this process, and the optimized image is presented in Figure 11c. The visual road schema of the optimized facility environment is extracted, and then the operation speed of the optimized facility environment is predicted with the trained random forest model. In addition to the original visual lane marking, the abundant landscape is added on both sides of the road. According to the visual sensitive schema, the added landscape reduces the operation speed by  $-16.78$  km/h, which satisfies the demand of the applicability indicator for visual sensitive schema in Table 4 (i.e.,  $[-40$  km/h,  $-15$  km/h]). As demonstrated in Figure 11d, the operation speed of the optimized facility environment is 48.89 km/h, less than the speed limit. The optimized facility environment images on all road sections with high tendencies of speeding are shown in Figure 12.

An additional case involving the optimization of multiple semantics within the facility environment is present in Figure 13. The visual semantic schema of this road section could be represented by the vector  $[0,0,0,0]$  and the visual sensitive schema vector of this road section is  $[0,0,0,0]$ . The speed limit is 50 km/h, and the optimization scheme for the original facility environment of the road section is determined to be  $[0,0,1,1]$ . This study transfers the speed revision ability of the landscape from Level 1 to Level 3 and the speed revision ability of the visual pulse from Level 1 to Level 2 to achieve the target operation speed.

In these cases, this method effectively optimizes these facility environments on speeding-prone road sections, where original operation speeds exceed the speed limit (more than 20% or even up to 45%). The whole optimization process takes around 1 h, far less than several months or years in previous ways. This intelligent optimization method has gained recognition and adoption by the local government and the Anhui Provincial Institute of Transportation Planning and Design.

## 10 | DISCUSSION

This study proposes an intelligent optimization method to optimize the facility environment on rural roads from drivers' visual perception, which could provide some useful insights for transportation departments. The automated approach for determining and verifying the optimization schemes of facility environments could alleviate the reliance on expert experience and human work. Besides, by generating visual images of the optimized facility environments and predicting the operation speeds, this study could provide transportation departments with a visual and quantitative representation of the

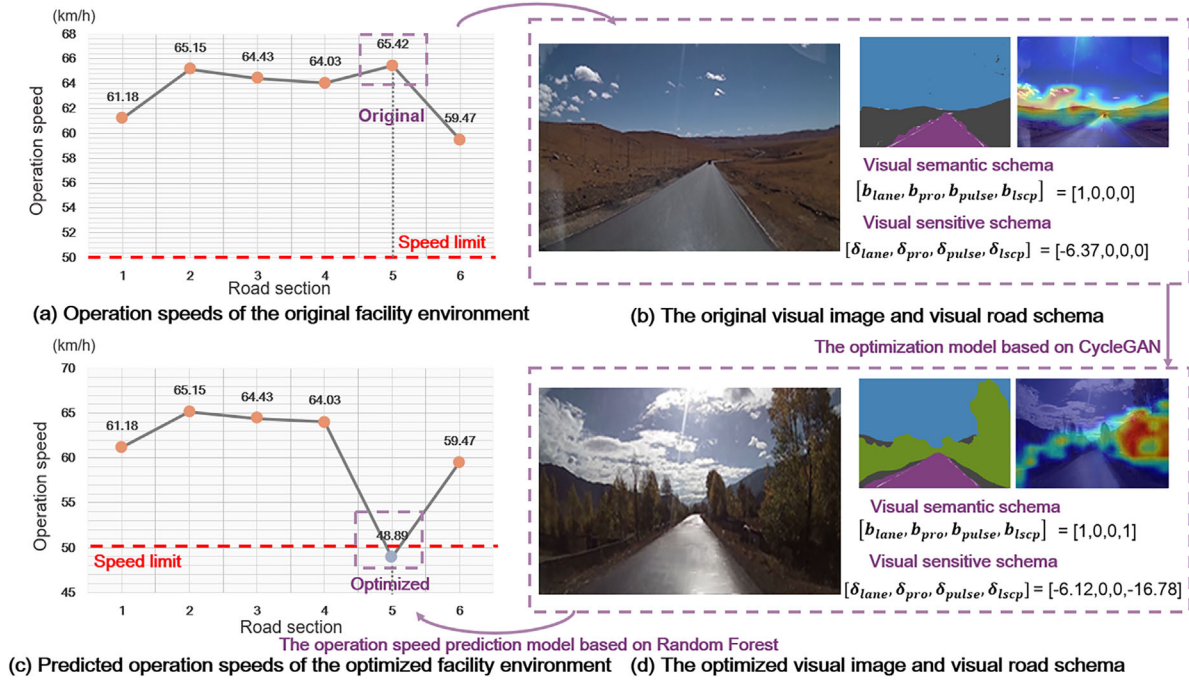


FIGURE 11 The optimization process of the selected road sections with high tendencies of speeding (an example of road section 5).

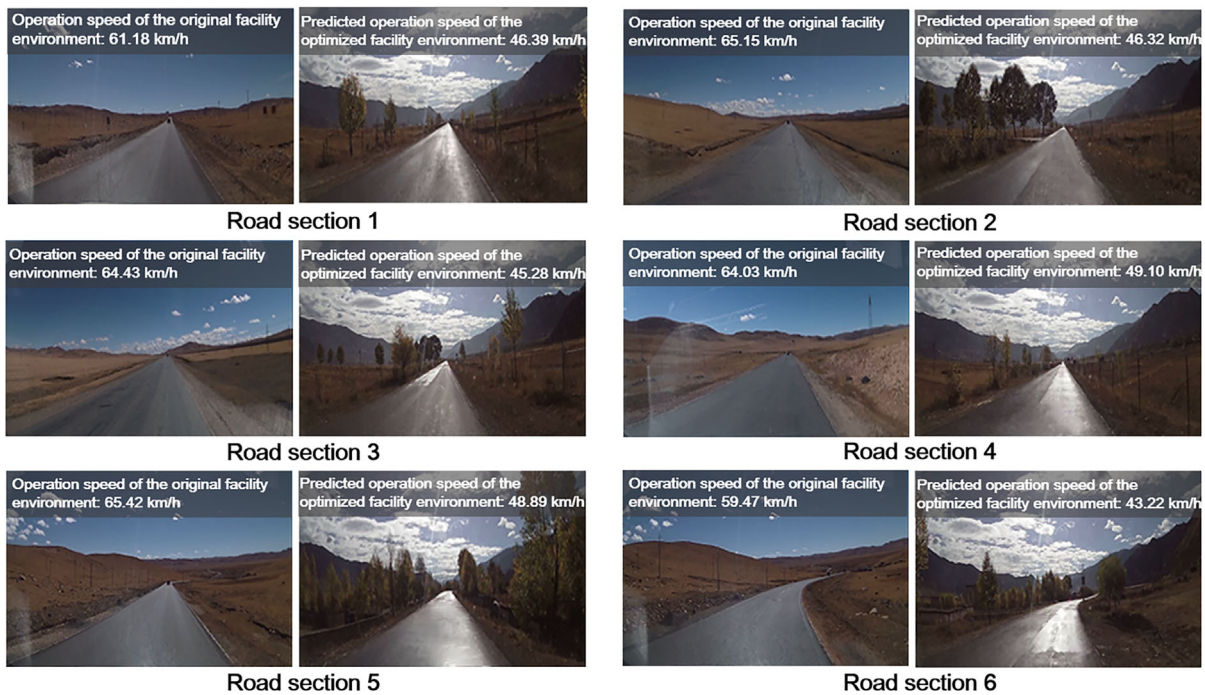


FIGURE 12 The optimized facility environment images of all road sections with high tendencies of speeding.

optimization outcomes. Compared with traditional optimization technology, it enhances the level of automation and intelligence in optimizing the facility environment on rural roads. In addition to two-way two-lane rural roads, this intelligent optimization method could also be applied to urban roads, expressways, and various other scenarios.

Drivers' visual perception has become increasingly essential in the design and optimization for the road facility environment (Fan Wang et al., 2020). However, the effectiveness of the facility environment design from drivers' visual perception needs to be verified by building virtual scenarios in driving simulators or conducting



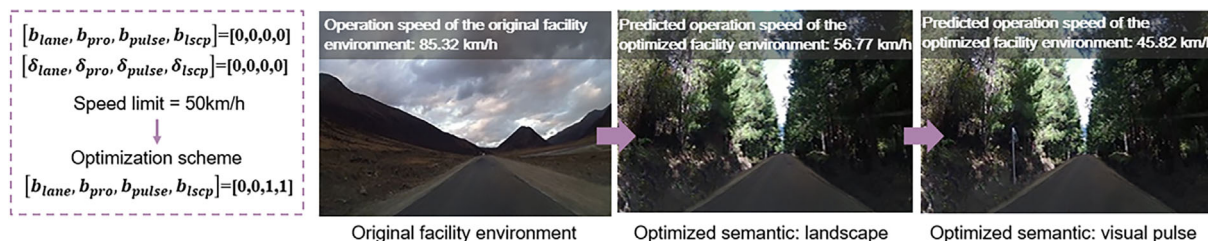


FIGURE 13 A case involving multiple semantic optimization.

driving experiments on real roads, which requires a lot of human and material resources (de Oña et al., 2014). Our optimization model based on CycleGAN could intelligently generate images of the designed facility environment through computers, which is a convenient and intuitionistic way to demonstrate design schemes. Combined with the random forest speed prediction model, the effect of road design or optimization could be reflected directly.

Furthermore, the facility environment generation and assessment technology from drivers' visual perception can offer insights for the efficient planning of road construction projects (Adeli & Karim, 2001). Combined with construction scheduling and management models, it allows for a more precise and cost-effective allocation of resources required for the development of road facility environments, leading to reduced construction costs (Karim & Adeli, 1999a, 1999b). Understanding how drivers visually perceive the facility environment is also crucial for developing intelligent transportation systems (ITS; Adeli & Karim, 2005). This knowledge can inform the development of advanced driver assistance systems, enhancing their ability to interpret and respond to visual cues (Badweeti et al., 2023). Combined with techniques such as traffic pattern detection (Karim & Adeli, 2002, 2003), traffic delay analysis (Jiang & Adeli, 2003), and congestion management (Adeli & Ghosh-Dastidar, 2004), it can contribute to a safer and more efficient ITS. Combined with nature-inspired algorithms, such as particle swarm optimization (Hossain et al., 2019), harmony search algorithm (Siddique & Adeli, 2015), simulated annealing (Siddique & Adeli, 2016), bacteria foraging algorithm (J. Wang et al., 2018), and spider monkey optimization (Akhand et al., 2020), this study can be extended to more complex traffic environments. These algorithms can help identify the most appropriate optimization methods for different traffic flow conditions, diverse road users, and traffic regulations (B. Liu et al., 2023).

Additionally, the optimization model could also be extended to autonomous driving. Due to the high requirements for the safety of autonomous driving, the object detection systems of autonomous vehicles need to be tested in many different scenarios (Zheng et al., 2018). However,

the available datasets could not cover enough possible situations (Junyao Guo et al., 2019). Our CycleGAN-based optimization model could generate artificial images of the facility environment with different scenario combinations according to needs, which could help increase the variety of scenarios and the coverage for testing.

Driving simulation has become a mainstream method in road testing and safety assessment because of its high degree of realism, low costs in experiments, adjustable experimental parameters (including vehicle, weather, and traffic), safety for test drivers, and accessible data collection (Wynne et al., 2019). The intelligent optimization technology proposed in this study could realize "design while simulated driving" (Gao et al., 2024). During the process of driving simulation, the facility environment from drivers' visual perception and the driving behavior could be synchronously collected. The road safety evaluation, optimization scheme generation, and facility environment optimization could be carried out in real time, and then the optimized visual images could be automatically generated.

There are a few limitations to this study. At present, the optimization model based on CycleGAN could not realize the simultaneous conversion of multiple objects and styles. If the optimization of the semantic and sensitive visual schemas involves more than one objective, it is necessary to optimize their content and features separately. Besides, in this study, elderly drivers (aged over 50) were not considered due to their limited presence on rural roads and distinct behavioral characteristics, compared to other drivers. With the increase in vehicle ownership rates among rural elderly individuals, corresponding methods tailored for elderly drivers to improve their safety on rural roads will be developed, such as driver assistance technologies and visual enhancement methods.

## 11 | CONCLUSION

This study aims to propose an intelligent optimization technology for the facility environment on rural roads to realize the process of road optimization from scheme design to effect verification. The visual road schema model,





including the visual semantic and sensitive schemas, is put forward to quantitatively quantify the facility environment from drivers' visual perception. Using self-explaining theory, the influences of the facility environment on operation speeds are analyzed, and the applicability and effectiveness indicators for the visual road schema are summarized to automatically determine the optimization scheme. Then, the CycleGAN-based image generation method is used to optimize the facility environment according to the optimization scheme. To verify the optimization effect, the operation speed prediction model based on the random forest algorithm is built. This optimization method has been applied to the selected road sections with high tendencies of speeding. It can effectively optimize these facility environments on these speeding-prone road sections, where original operation speeds exceed the speed limit (more than 20% or even up to 45%). The whole optimization process takes around 1 h, far less than several months or years in previous ways. This study elevates the intelligence level in optimizing the facility environment and contributes to the improvement of rural road safety.

## ACKNOWLEDGMENTS

This project was jointly supported by the National Natural Science Foundation of China (52102416) and the National Science Foundation of Shanghai (22ZR1466000) Area of Advance Transport, Chalmers University of Technology.

## REFERENCES

- Adeli, H., & Karim, A. (2001). *Construction scheduling, cost optimization, and management—A new model based on neurocomputing and object technologies*. Spon Press.
- Adeli, H., & Ghosh-Dastidar, S. (2004). Mesoscopic-wavelet freeway work zone flow and congestion feature extraction model. *Journal of Transportation Engineering*, 130(1), 94–103.
- Adeli, H., & Karim, A. (2005). *Wavelets in intelligent transportation systems*. John Wiley & Sons, Inc.
- Akhand, M. A. H., Ayon, S. I., Shahriyar, S. A., Siddique, N., & Adeli, H. (2020). Discrete spider monkey optimization for travelling salesman problem. *Applied Soft Computing*, 86, 105887.
- Almahairi, A., Rajeshwar, S., Sordoni, A., Bachman, P., & Courville, A. (2018). Augmented CycleGan: Learning many-to-many mappings from unpaired data. In International Conference on Machine Learning, Stockholm, Sweden (pp. 195–204).
- Alzubaidi, L., Zhang, J., Humaidi, A. J., Al-Dujaili, A., Duan, Y., Al-Shamma, O., Santamaría, J., Fadhel, M. A., Al-Amidie, M., & Farhan, L. (2021). Review of deep learning: Concepts, CNN architectures, challenges, applications, future directions. *Journal of Big Data*, 8, 53.
- Ambros, J., Elgner, J., Turek, R., & Valentova, V. (2020). Where and when do drivers speed? A feasibility study of using probe vehicle data for speeding analysis. *Archives of Transport*, 53(1), 103–113.
- Ambros, J., Valentová, V., Gogolín, O., Andrášik, R., Kubeček, J., & Bíl, M. (2017). Improving the self-explaining performance of Czech national roads. *Transportation Research Record*, 2635(1), 62–70.
- Ambunda, R., & Sinclair, M. (2022). Traffic safety and the rural road environment: Assessing the impact of combined roadway conditions on crash incidence. *Journal of the South African Institution of Civil Engineering*, 64(4), 38–48.
- Antonson, H., Ahlström, C., Mårdh, S., Blomqvist, G., & Wiklund, M. (2014). Landscape heritage objects' effect on driving: A combined driving simulator and questionnaire study. *Accident Analysis & Prevention*, 62, 168–177.
- Babić, D., & Brijs, T. (2021). Low-cost road marking measures for increasing safety in horizontal curves: A driving simulator study. *Accident Analysis & Prevention*, 153, 106013.
- Badweeti, K. N., Malaghan, V. D., Pawar, D. S., & Easa, S. (2023). Evaluating effectiveness and acceptance of advanced driving assistance systems using field operational test. *Journal of Intelligent and Connected Vehicles*.
- Bella, F. (2013). Driver perception of roadside configurations on two-lane rural roads: Effects on speed and lateral placement. *Accident Analysis & Prevention*, 50, 251–262.
- Broughton, P. S., Fuller, R., Stradling, S., Gormley, M., Kinnear, N., O'dolan, C., & Hannigan, B. (2009). Conditions for speeding behaviour: A comparison of car drivers and powered two wheeled riders. *Transportation Research Part F: Traffic Psychology and Behaviour*, 12(5), 417–427.
- Charlton, S. G., & Starkey, N. J. (2017). Driving on urban roads: How we come to expect the 'correct' speed. *Accident Analysis & Prevention*, 108, 251–260.
- Charlton, S. G., Mackie, H. W., Baas, P. H., Hay, K., Menezes, M., & Dixon, C. (2010). Using endemic road features to create self-explaining roads and reduce vehicle speeds. *Accident Analysis & Prevention*, 42(6), 1989–1998.
- Chen, Y., Xie, X., Yu, B., Li, Y., & Lin, K. (2021). Multitarget vehicle tracking and motion state estimation using a novel driving environment perception system of intelligent vehicles. *Journal of Advanced Transportation*, 2021, 6251399.
- Coakley, R., Storm, R., & Neuman, T. (2016). Relationship between geometric design features and performance. *Transportation Research Record*, 2588(1), 80–88.
- Cox, J. A., Beanland, V., & Filtress, A. J. (2017). Risk and safety perception on urban and rural roads: Effects of environmental features, driver age and risk sensitivity. *Traffic Injury Prevention*, 18(7), 703–710.
- Cruzado, I., & Donnell, E. T. (2010). Factors affecting driver speed choice along two-lane rural highway transition zones. *Journal of Transportation Engineering*, 136(8), 755–764.
- de Oña, J., de Oña, R., Eboli, L., Forciniti, C., & Mazzulla, G. (2014). How to identify the key factors that affect driver perception of accident risk. A comparison between Italian and Spanish driver behavior. *Accident Analysis & Prevention*, 73, 225–235.
- Du, Z. G., Tang, Y. H., Xie, J., & Li, P. F. (2018). New research on improved highway tunnel based on visual illusion. *CICTP 2017: Transportation reform and change—Equity, inclusiveness, sharing, and innovation*, Shanghai, China (pp. 4369–4379).
- EU Road Safety Statistics. (2019). Road safety statistics: What is behind the figures? European Commission. [https://ec.europa.eu/commission/presscorner/detail/en/qanda\\_20\\_1004](https://ec.europa.eu/commission/presscorner/detail/en/qanda_20_1004)
- Galante, F., Mauriello, F., Montella, A., Perneti, M., Aria, M., & D'Ambrosio, A. (2010). Traffic calming along rural highways crossing small urban communities: Driving simulator experiment. *Accident Analysis & Prevention*, 42(6), 1585–1594.



- Gao, J., Yu, B., Chen, Y., Bao, S., Gao, K., & Zhang, L. (2024). An ADAS with better driver satisfaction under rear-end near-crash scenarios: A spatio-temporal graph transformer-based prediction framework of evasive behavior and collision risk. *Transportation Research Part C: Emerging Technologies*, 159, 104491.
- Gatys, L. A., Ecker, A. S., & Bethge, M. (2016). Image style transfer using convolutional neural networks. Proceedings of the IEEE Conference on Computer Vision and Pattern Recognition, Las Vegas, NV (pp. 2414–2423).
- Gayah, V. V., & Donnell, E. T. (2021). Estimating safety performance functions for two-lane rural roads using an alternative functional form for traffic volume. *Accident Analysis & Prevention*, 157, 106173.
- Ghorbani, M., Saffarzadeh, M., & Naderan, A. (2023). Crash prediction modeling for horizontal curves on two-lane, two-way rural highways based on consistency and self-explaining characteristics using zero-truncated data. *KSCE Journal of Civil Engineering*, 27, 3567–3580.
- Goldenbeld, C., & van Schagen, I. (2007). The credibility of speed limits on 80 km/h rural roads: The effects of road and person (ality) characteristics. *Accident Analysis & Prevention*, 39(6), 1121–1130.
- Guo, J., Kurup, U., & Shah, M. (2019). Is it safe to drive? An overview of factors, metrics, and datasets for driveability assessment in autonomous driving. *IEEE Transactions on Intelligent Transportation Systems*, 21(8), 3135–3151.
- Guo, J., Wang, Q., & Li, Y. (2021). Semi-supervised learning based on convolutional neural network and uncertainty filter for façade defects classification. *Computer-Aided Civil and Infrastructure Engineering*, 36(3), 302–317.
- Hallmark, S. L., Hawkins, N., Fitzsimmons, E., Resler, J., Plazak, D., Welch, T., & Petersen, E. (2008). Use of physical devices for calming traffic along major roads through small rural communities in Iowa. *Transportation Research Record*, 2078(1), 100–107.
- He, K., Zhang, X., Ren, S., & Sun, J. (2016). Deep residual learning for image recognition. Proceedings of the IEEE Conference on Computer Vision and Pattern Recognition, Las Vegas, NV (pp. 770–778).
- He, L., Yu, B., Chen, Y., Bao, S., Gao, K., & Kong, Y. (2023). An interpretable prediction model of illegal running into the opposite lane on curve sections of two-lane rural roads from drivers' visual perceptions. *Accident Analysis & Prevention*, 186, 107066.
- Herrstedt, L. (2006). Self-explaining and forgiving roads: speed management in rural areas. In Proceedings: ARRB Group Biennial Conference (Vol. 22, No. CD-ROM). ARRB Group.
- Hossain, S. I., Akhand, M. A. H., Shuvo, M. I. R., Siddique, N., & Adeli, H. (2019). Optimization of university course scheduling problem using particle swarm optimization with selective search. *Expert Systems with Applications*, 127, 9–24.
- Hou, W., Lyu, N., Liu, Z., & Wang, X. (2020). Modelling large vehicles operating speed characteristics on freeway alignment based on aggregated GPS data. *IET Intelligent Transport Systems*, 14(8), 857–865.
- Isola, P., Zhu, J. Y., Zhou, T., & Efros, A. A. (2017). Image-to-image translation with conditional adversarial networks. Proceedings of the IEEE Conference on Computer Vision and Pattern Recognition, Honolulu, HI (pp. 1125–1134).
- Jiang, X., & Adeli, H. (2003). Freeway work zone traffic delay and cost optimization model. *Journal of Transportation Engineering*, 129(3), 230–241.
- Job, R. S., & Brodie, C. (2022). Road safety evidence review: Understanding the role of speeding and speed in serious crash trauma: A case study of New Zealand. *Journal of Road Safety*, 33(1), 5–25.
- Kapsky, D., Bogdanovich, S., & Volynets, A. (2020). Implementation of the road traffic safety concept in Belarus. In A. Varhelyi, V. Žuraulis, & O. Prentkovskis (Eds.), *Vision zero for sustainable road safety in Baltic Sea region: Proceedings of the international conference "vision zero for sustainable road safety in Baltic Sea region"* (pp. 110–119). Springer International Publishing.
- Karim, A., & Adeli, H. (1999a). OO Information model for construction project management. *Journal of Construction Engineering and Management*, 125(5), 361–367.
- Karim, A., & Adeli, H. (1999b). CONSCOM: An OO construction scheduling and change management system. *Journal of Construction Engineering and Management*, 125(5), 368–376.
- Karim, A., & Adeli, H. (2002). Incident detection algorithm using wavelet energy representation of traffic patterns. *Journal of Transportation Engineering*, 128(3), 232–242.
- Karim, A., & Adeli, H. (2003). Fast automatic incident detection on urban and rural freeways using wavelet energy algorithm. *Journal of Transportation Engineering*, 129(1), 57–68.
- Karlsson, S., & Welander, P. (2018). Generative adversarial networks for image-to-image translation on street view and MR images. <https://www.diva-portal.org/smash/record.jsf?dswid=8273&pid=diva2%3A1216606>
- Kim, T. K. (2017). Understanding one-way ANOVA using conceptual figures. *Korean Journal of Anesthesiology*, 70(1), 22–26.
- Kingma, D. P., & Ba, J. (2014). Adam: A method for stochastic optimization. arXiv preprint. arXiv:1412.6980. <https://arxiv.org/abs/1412.6980>
- Kwak, D. H., & Lee, S. H. (2020). A novel method for estimating monocular depth using cycle GAN and segmentation. *Sensors*, 20(9), 2567.
- Liu, B., Liu, X., Yang, Y., Chen, X., & Ma, X. (2023). Resilience assessment framework toward interdependent bus–rail transit network: Structure, critical components, and coupling mechanism. *Communications in Transportation Research*, 3, 100098.
- Liu, H. (2013). Analysis of intersection accidents of mountainous highway. *Procedia-Social and Behavioral Sciences*, 96, 205–209.
- Liu, P., Huang, J., Wang, W., & Xu, C. (2011). Effects of transverse rumble strips on safety of pedestrian crosswalks on rural roads in China. *Accident Analysis & Prevention*, 43(6), 1947–1954.
- Ma, J., Gu, J., Jia, H., Yao, Z., & Chang, R. (2018). The relationship between drivers' cognitive fatigue and speed variability during monotonous daytime driving. *Frontiers in Psychology*, 9, 459.
- MacFarland, T. W., & Yates, J. M. (2016). Kruskal–Wallis H-test for one way analysis of variance (ANOVA) by ranks. In T. W. MacFarland & J. M. Yates (Eds.), *Introduction to nonparametric statistics for the biological sciences using R* (pp. 177–211). Springer.
- Mackie, H., Brodie, C., Scott, R., Hirsch, L., Tate, F., Russell, M., & Holst, K. (2017). The signs they are a-changin': Development and evaluation of New Zealand's rural intersection active warning system. *Journal of the Australasian College of Road Safety*, 28(3), 11–21.
- Mahmud, M. S., Megat Johari, M. U., Bamney, A., Jashami, H., Gates, T. J., & Savolainen, P. T. (2023). Driver response to a dynamic speed feedback sign at speed transition zones along high-speed rural highways. *Transportation Research Record*, 2677(2), 1341–1353.



- Marshall, W. E., & Ferenchak, N. N. (2017). Assessing equity and urban/rural road safety disparities in the US. *Journal of Urbanism: International Research on Placemaking and Urban Sustainability*, 10(4), 422–441.
- Montella, A., Aria, M., D'Ambrosio, A., Galante, F., Mauriello, F., & Perneti, M. (2011). Simulator evaluation of drivers' speed, deceleration and lateral position at rural intersections in relation to different perceptual cues. *Accident Analysis & Prevention*, 43(6), 2072–2084.
- Montella, A., Galante, F., Mauriello, F., & Pariota, L. (2015). Effects of traffic control devices on rural curve driving behavior. *Transportation Research Record*, 2492(1), 10–22.
- National Highway Traffic Safety Administration. (2022a). *Overview of motor vehicle crashes in 2020* (Report No. DOT HS 813 266). National Highway Traffic Safety Administration.
- National Highway Traffic Safety Administration. (2022b). *Rural-urban comparison of motor vehicle traffic fatalities* (Traffic Safety Facts. Report No. DOT HS 813 488). National Highway Traffic Safety Administration.
- Naveen, N., Rajesh, M., Srinivas, M., & Fasiuddin, M. (2017). Road safety audit of a rural road. *International Journal of Civil Engineering and Technology (IJCIET)*, 8(4), 752–761.
- Pasindu, H. R., Ranawaka, R. K. T. K., Sandamal, R. M. K., & Dias, T. W. K. I. M. (2021). Incorporating road safety into rural road network pavement management. *International Journal of Pavement Engineering*, 23(12), 4306–4319.
- Persaud, B. N., Retting, R. A., & Lyon, C. A. (2004). Crash reduction following installation of centerline rumble strips on rural two-lane roads. *Accident Analysis & Prevention*, 36(6), 1073–1079.
- Qin, Y., Chen, Y., & Lin, K. (2020). Quantifying the effects of visual road information on drivers' speed choices to promote self-explaining roads. *International Journal of Environmental Research and Public Health*, 17(7), 2437.
- Shaaban, K., Mohammad, A., & Eleimat, A. (2023). Effectiveness of a fixed speed camera traffic enforcement system in a developing country. *Ain Shams Engineering Journal*, 14(10), 102154.
- Shao, X., Wei, C., Shen, Y., & Wang, Z. (2020). Feature enhancement based on CycleGAN for nighttime vehicle detection. *IEEE Access*, 9, 849–859.
- Siddique, N., & Adeli, H. (2015). Harmony search algorithm and its variants. *International Journal of Pattern Recognition and Artificial Intelligence*, 29(8), 1539001.
- Siddique, N., & Adeli, H. (2016). Simulated annealing, its variants and engineering applications. *International Journal on Artificial Intelligence Tools*, 25(6), 1630001.
- Theeuwes, J. (2021). Self-explaining roads: What does visual cognition tell us about designing safer roads? *Cognitive Research: Principles and Implications*, 6(1), 15.
- Theeuwes, J., & Godthelp, H. (1995). Self-explaining roads. *Safety Science*, 19(2-3), 217–225.
- Theeuwes, J., & van der Horst, R. (2017). *Designing safe road systems: A human factors perspective*. CRC Press.
- Traffic Administration Bureau of the Ministry of Public Security of PRC. (2020). China road traffic accidents statistics. <https://www.mps.gov.cn/>
- Turner, B., Makwasha, T., & Hillier, P. (2017). Infrastructure treatments for managing speeds on rural and urban arterial roads. *Journal of Road Safety*, 28(2), 13–20.
- Van Treese, J. W., II, Koester, A. K., Fitzpatrick, G. E., Olexa, M. T., & Allen, E. J. (2017). A review of the impact of roadway vegetation on drivers' health and well-being and the risks associated with single-vehicle crashes. *Arboricultural Journal*, 39(3), 179–193.
- Vignali, V., Bichicchi, A., Simone, A., Lantieri, C., Dondi, G., & Costa, M. (2019). Road sign vision and driver behaviour in work zones. *Transportation Research Part F: Traffic Psychology and Behaviour*, 60, 474–484.
- Wager, S., & Athey, S. (2018). Estimation and inference of heterogeneous treatment effects using random forests. *Journal of the American Statistical Association*, 113(523), 1228–1242.
- Walker, G. H., Stanton, N. A., & Chowdhury, I. (2013). Self-explaining roads and situation awareness. *Safety Science*, 56, 18–28.
- Wang, F., & Chen, F. (2011). Influencing factor analysis for visual information search while driving: Based on modeling of visually interesting regions. In ICCTP 2011: Towards Sustainable Transportation Systems (pp. 2534–2544).
- Wang, F., Chen, Y., Wijnands, J. S., & Guo, J. (2020). Modeling and interpreting road geometry from a driver's perspective using variational autoencoders. *Computer-Aided Civil and Infrastructure Engineering*, 35(10), 1148–1159.
- Wang, J., Zhong, D., Adeli, H., Wang, D., & Liu, M. (2018). Smart bacteria-foraging algorithm-based customized kernel support vector regression and enhanced probabilistic neural network for compaction quality assessment and control of earth-rock dam. *Expert Systems*, 35(6), e12357.
- Weber, R., & Hartkopf, G. (2005). New Design Guidelines—A Step Towards Self-Explaining Roads? In 3rd International Symposium on Highway Geometric Design Transportation Research Board American Association of State Highway and Transportation Officials (AASHTO) Federal Highway Administration American Society of Civil Engineers Association Mondiale de la Route International Road Federation Institute of Transportation Engineers (ITE) National Association of County Engineers Transportation Association of Canada (TAC) Chicago Department of Transportation Illinois Department of Transportation Illinois State Toll Highway Authority.
- Wynne, R. A., Beanland, V., & Salmon, P. M. (2019). Systematic review of driving simulator validation studies. *Safety Science*, 117, 138–151.
- Xu, M., Di, Y., Ding, H., Zhu, Z., Chen, X., & Yang, H. (2023). AGNP: Network-wide short-term probabilistic traffic speed prediction and imputation. *Communications in Transportation Research*, 3, 100099. <https://doi.org/10.1016/j.commtr.2023.100099>
- Xu, Y., Ye, Z., & Wang, C. (2021). Modeling commercial vehicle drivers' acceptance of advanced driving assistance system (ADAS). *Journal of Intelligent and Connected Vehicles*, 4(3), 125–135.
- Yang, Y., Ng, S. T., Dao, J., Zhou, S., Xu, F. J., Xu, X., & Zhou, Z. (2021). BIM-GIS-DCEs enabled vulnerability assessment of interdependent infrastructures—A case of stormwater drainage-building-road transport Nexus in urban flooding. *Automation in Construction*, 125, 103626.
- Yu, B., Chen, Y., & Bao, S. (2019). Quantifying visual road environment to establish a speeding prediction model: an examination using naturalistic driving data. *Accident Analysis & Prevention*, 129, 289–298.



- Yu, B., Chen, Y., Bao, S., & Xu, D. (2018). Quantifying drivers' visual perception to analyze accident-prone locations on two-lane mountain highways. *Accident Analysis & Prevention*, *119*, 122–130.
- Yuan, A., Changcheng, L., & Zhang, G. (2012). GRSP/MOT speed management pilot project in China. Australasian Road Safety Research, Policing and Education Conference, Wellington, New Zealand.
- Zheng, X., Huang, B., Ni, D., & Xu, Q. (2018). A novel intelligent vehicle risk assessment method combined with multi-sensor fusion in dense traffic environment. *Journal of Intelligent and Connected Vehicles*, *1*(2), 41–54.
- Zhong, C., Wu, P., Zhang, Q., & Ma, Z. (2023). Online prediction of network-level public transport demand based on principle component analysis. *Communications in Transportation Research*, *3*, 100093.
- Zhu, J. Y., Park, T., Isola, P., & Efros, A. A. (2017). Unpaired image-to-image translation using cycle-consistent adversarial networks. Proceedings of the IEEE International Conference on Computer Vision, Venice, Italy (pp. 2223–2232).

**How to cite this article:** Ren, W., Yu, B., Chen, Y., Gao, K., Bao, S., Wang, Z., & Qin, Y. (2024). An intelligent optimization method for the facility environment on rural roads. *Computer-Aided Civil and Infrastructure Engineering*, 1–22.  
<https://doi.org/10.1111/mice.13209>





## APPENDIX

















Visual semantic schema <i>blane,bpro,bpulse,blscp</i>	<i>V</i> (km/h)	<i>SD</i> (km/h)	Visual semantic schema <i>blane,bpro,bpulse,blscp</i>	<i>V</i> (km/h)	<i>SD</i> (km/h)
	63.18	3.52		48.30	3.03
[0,0,0,0]			[1,0,0,1]		
	61.49	3.21		47.95	3.45
[1,0,0,0]			[1,0,1,1]		
	56.69	3.47		51.94	2.88
[0,0,1,0]			[1,1,0,0]		
	55.14	3.54		43.01	3.42
[1,0,1,0]			[0,0,1,1]		
	49.80	3.21		42.66	3.62
[1,1,1,1]			[0,0,0,1]		
	45.84	3.52		39.60	3.68
[1,1,0,1]			[0,1,0,1]		
	50.52	3.38		48.72	3.54
[1,1,1,0]			[0,1,1,0]		
	53.17	3.03		34.29	3.34
[0,1,0,0]			[0,1,1,1]		

FIGURE A1 Statistical values of operation speeds of different visual semantic schemas.